ce/papers Proceedings in civil engineering

Ernst & Sohn A Wiley Brand

Check for updates

ORIGINAL ARTICLE

eurosteel AMSTERDAM 2023

Ernst & Sohn A Wiley Brand

Wire-and-Arc Additive Manufacturing for lattice steel structures: overview of the experimental characterization on dot-by-dot rods

Lidiana Arrè[1] | Vittoria Laghi[1] | Michele Palermo[1] | Giada Gasparini[1] | Tomaso Trombetti[1]

Correspondence

Dr. Vittoria Laghi PhD
University of Bologna
Department of Civil, Chemical, Environmental and Materials Engineering
Viale del Risorgimento 2
40136 Bologna, Italy
Email: vittoria.laghi2@unibo.it

[1] Department of Civil, Chemical, Environmental and Materials Engineering, University of Bologna, Bologna, Italy

Abstract

With the advent of a new arc-based additive manufacturing (AM) process, referred to as Wire-and-Arc Additive Manufacturing (WAAM), the scale of the metal printed parts increased up to several meters, thus becoming suitable for large-scale applications in marine, aerospace and construction sectors. However, specific considerations in terms of geometrical and mechanical properties ought to be made in order to effectively use the printed outcomes for structural engineering purposes. The introduction of the novel printing strategy referred to as "dot-by-dot", consisting in successive drops of molten metal, enabled the use of WAAM to realize complex lattice structures, made by continuous grids of WAAM rods. Nevertheless, their proper design requires an accurate evaluation of the influence of the non-negligible inherent geometrical irregularities on the mechanical response of the rods. Hence, extensive experimental work is needed in order to evaluate the mechanical response of "dot-by-dot" WAAM rods with geometrical imperfections. The present study focuses on the mechanical characterization of dot-by-dot WAAM-produced 304L stainless steel intersected rods, constituting the basic units of grid and lattice structures. The mechanical response of the specimens is assessed through tensile experimental tests conducted on two-ways planar nodes obtained from the intersection of two rods with different angles, hereafter also refereed to as crossed rods. The experimental results are then compared with tensile tests on single rods, to quantify the influence of the intersection angle in the structural response of the lattice structures.

Keywords

Directed Energy Deposition; Experimental tests; Stainless steel.

1 Introduction

The 4th Industrial Revolution has brought new digital manufacturing technologies and materials, essential to enable a more efficient and CO_2-neutral construction, accounting for individualized and sustainable outcomes with better performances.

Additive Manufacturing (AM) technologies have been adopted in pioneering applications in the construction sector. Among different AM technologies, Directed Energy Deposition (DED), and in particular Wire-and-Arc Additive Manufacturing (WAAM), demonstrated to be the most suitable to realize large-scale metal outcomes, enabling the "out-of-the-box" fabrication with ideal no constraints in terms of geometry, shape and dimensions [1–4]. The possibility of manufacturing WAAM outcomes up to several meters of span demonstrated the potential use of this technology to fabricate steel structures [5, 6]. The combination of WAAM technology with computational design tools for free-form design could also allow the realisation of new optimized structures [7, 8]. However, the reliable design of WAAM structures must be based on the knowledge of the main mechanical properties of the elements, which are largely influenced by the WAAM process parameters, microstructure and inherent geometrical irregularities of the printed pieces. The present study aims at providing the first results of a wide research work aimed at assessing the mechanical response of "dot-by-dot" WAAM-produced steel lattice structures. Section 2 introduces the structural potential of WAAM-produced lattice elements. Section 3 presents the main results of the experimental work, while considerations on future work are drawn in Section 4.

2 WAAM for lattice steel structures

WAAM-produced outcomes may be realized by adopting one of the currently known printing deposition strategies:

(i) "continuous" printing, a layer-by-layer deposition, suitable to realize planar geometries, (ii) "dot-by-dot" printing, consisting in a droplet's deposition, suitable to realize rod-like elements, constituting the basic units of grid and lattice structures.

Currently, the interest in the "dot-by-dot" strategy is growing, allowing the realization of structural elements, such as free-form gridshells, lattice structures and application of steel rods as reinforcement for innovative 3D-printed concrete structures [9] (Figure 1). Therefore, there is an increasing need in the assessment of the mechanical properties of WAAM-produced steel rods, which may differ with respect to those of WAAM-produced "continuous" specimens [10–12].

The design of steel lattice structures requires detailed knowledge of the mechanical response of WAAM-produced steel rods, taking into account various aspects, such as (1) the inherent geometrical irregularities (such as surface roughness, lack of straightness, cross-section variation), (2) the influence of the inclination of the build angles (referring to the angle between the axis of the WAAM rod and the vertical axis, perpendicular to the base platform) and nozzle angles (referring to the inclination of the nozzle with respect to the printed rod), (3) the presence of the nodes in the connected rods.

Figure 1 Possible structural application of a "dot-by-dot" WAAM-produced diagrid lattice structure

3 Experimental characterization

The present section provides an overview of the main result of the experimental investigation on single rods and crossed rods carried out at the structural testing lab of the University of Bologna. The aim is to study the mechanical response of "dot-by-dot" WAAM-produced stainless steel basic components of a WAAM lattice structure, e.g. inclined single rods and nodes (Figure 2). The influence of the build angle and nodal region on the mechanical response of the printed rods has been investigated by considering different build angles for both single and crossed rods, between the two limit cases of 0° and 45° build angles, corresponding to the limit conditions for printable structural applications. The mechanical response was studied under different loading conditions: tension, compression and bending [13]. The different experimental tests allow the assessment of the key mechanical properties of WAAM-produced lattice structures in construction applications. The mechanical tests were carried out on as-built rods, hence not subjected to post-processing milling treatments, to account for the influence of the surface roughness and other geometrical irregularities, as for the case of real applications in construction.

The tested WAAM-produced rods were manufactured adopting the specific values of the printing process parameters based on the know-how of the manufacturing company MX3D [14]. The wire used for the printing process was the commercially available standard stainless steel welding wire grade ER308LSi (1 mm diameter) supplied by Oerlikon.

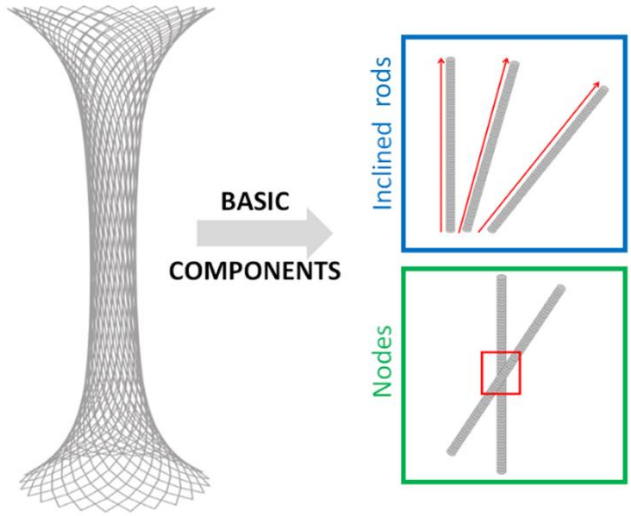

Figure 2 Diagrid lattice structure and its basic components: inclined single rods and nodes

3.1 Geometrical characterization

Generally speaking, "dot-by-dot" WAAM-produced rods are characterized by a non-uniform circular cross-section and lack of straightness of the longitudinal axis, resulting in structural eccentricities and secondary bending stresses even when subjected to axial force only. Nevertheless, given the non-uniform geometrical properties of the rods, for structural design purposes, it is possible to make use of a simplified approach grounded on effective mechanical parameters, based on an ideal cylinder of uniform along-the-length cross sectional area (A_{eff}) having the same volume of the actual rod (Figure 3). According to this equivalent geometrical model, it is possible to study the behavior of a "dot-by-dot" WAAM rod according to the Euler beam theory and the effective mechanical parameters . In particular, the effective axial tensile stress associated with a tensile force F can be computed as $\sigma_{eff} = \frac{F}{A_{eff}}$

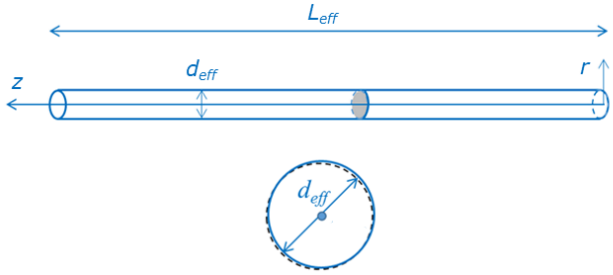

Figure 3 Effective cross-section for WAAM-produced rods

3.2 Single rods under tensile loading

The first batch of WAAM-produced steel single rods was tested in tension, considering 3 different build angles: 10 rods with 0° build angle (dot-0), 10 rods with 10° build angle (dot-10), 9 rods with 45° build angle (dot-45).

The tensile tests were performed at the Structural Engineering lab of the University of Bologna. The experimental set-up consisted of a Universal testing machine of 500 kN load capacity. The rods were tested in displacement control with a velocity corresponding to a stress rate of 2MPa/s. The strains were measured by adopting two types of monitoring systems: (1) a linear deformometer with a nominal dimension of 50 mm to detect the linear deformation of the rod up to yielding, and (2) an optical-based system, named Digital Image Correlation (DIC), to acquire information on the full strain field during the whole tensile test up to the failure point.

The following key effective mechanical parameters were estimated: Young's modulus (E), 0.2% proof stress ($R_{p0.2}$) and ultimate tensile strength (UTS), yielding strain (ε_y) and ultimate strains (ε_u), elongation at rupture (A%), ductility ($\mu_e = \varepsilon_u/\varepsilon_y$). The reader is referred to Ref. [13] for the detailed definitions and the experimental evaluation of the key effective mechanical parameters. Table 1 summarizes the main results (mean values and standard deviations) obtained from the tests. Most of the key effective parameters show decreasing average values for increasing build angles. However, they also present coefficients of variation with values up to 0.12 for the ultimate tensile strength and 0.28 for Young's modulus. The values of 0.2% proof stress and ultimate tensile strength are comparable with those of traditionally manufactured 304L stainless steel, whereas Young's modulus values (around 100 GPa) are much lower, as already observed when considering specimens extracted from WAAM-produced stainless steel plates manufactured using the "continuous" printing strategy [12].

Table 1 Summary of key effective tensile mechanical parameters of WAAM-produced single rods

Specimen ID	E [GPa]	$R_{p0.2}$ [MPa]	UTS [MPa]	$A_{\%}$ [%]	$R_{p0.2}$/UTS [-]	μ_e [-]
dot-0	133 ± 27	243 ± 20	524 ± 56	35 ± 14	0.47 ± 0.03	93 ± 42
dot-10	108 ± 19	245 ± 21	536 ± 49	34 ± 9	0.46 ± 0.03	79 ± 21
dot-45	98 ± 28	208 ± 20	419 ± 29	24 ± 6	0.50 ± 0.05	55 ± 14

3.3 Single rods under flexure and compression loading

A further batch of WAAM-produced single rods with 0° build angle was also tested under flexural (three-point bending) and compression loading. A total number of 10 rods of 250 mm in length were tested by means of three-point bending tests within their elastic range to assess the flexural Young's modulus. Then, the same rods were tested under compression.

The three-point bending test set-up consisted of two fixed steel cylindrical supports at 200 mm to obtain the simple support end restraints, while a concentrated load has been applied at the mid-span of the rod through another steel cylinder acting in displacement control with a velocity of 2 mm/min until the target displacement (corresponding to the elastic limit based on the tensile tests results [13]) was reached. The effective flexural elastic modulus resulted roughly equal to 85% of the effective Young's modulus as evaluated from the tensile tests on 0° build angle rods.

Then, the rods at 0° build angle were tested under compression loading, considering different effective buckling lengths to evaluate the behavior in compression for different slenderness levels (from stocky to slender specimens). The tests were performed in displacement control with the rod constrained having partially doubly fixed end restraints, resulting in an effective length buckling factor β of around 0.9. As expected, the response of the tested rods showed a progressive reduction of the ultimate compression strength for increasing level of slenderness, following the trends of the buckling curves for conventional steel members, see e.g. Eurocode 3 (EC3) [15].

3.4 Crossed rods under tensile loading

WAAM-produced steel crossed rods were manufactured considering three different intersection angles, e.g. 10°, 20°, 30°, nominal diameter of 6 mm and rod length of 260 mm (Figure 4). The experimental tests on these specimens were planned to study the mechanical response of the rods under tensile loading due to the influence of the intersection, referred to as nodal region.

The three batches of WAAM-produced crossed rods with three different build angles were tested in traction to assess the influence of the nodal area and intersection angle (e.g. the build angle of rod B) on the tensile behavior. For this aim, the crossed rods were manufactured in order to have one vertical rod, printed with a build angle of 0°, referred to as rod A, and one inclined rod, printed at a certain build angle based on the different batch, referred to as rod B, with angles respectively of 10°, 20° and 30° (Figure 5). The three batches are referred to as X10, X20, and X30. For some specimens of each batch, a first series of tensile tests were performed by applying the tensile force on type-A rods, after having cut the two end portions of the type-B rods. Then two other tensile tests were performed on the two type B rods cut from the initial specimen. Thus for each specimen, a total of three tensile tests were performed. This first testing procedure is referred to as Procedure A. For the remaining specimens of each batch the same protocol has been carried out, but inverting the type-A rods with the type-B rods. This second testing procedure is referred to as Procedure B.

A total number of 43 WAAM-produced specimens were manufactured, 15 of type X10 (8 following Procedure A, 7 following Procedure B), 15 of type X20 (8 following Procedure A, 7 following Procedure B), and 13 of type X30 (7 following Procedure A, 6 following Procedure B). The tensile tests were performed using the same testing machine and the same loading condition of the single rods presented in Section 3.2. The deformations of the specimens

were monitored through one deformometer with gauge length of 50 mm positioned across the nodal region, and one deformometer with gauge length of 25 mm positioned within the rod region (Figure 6).

Figure 7 reports the bar chart related to the ultimate tensile force (F_u) derived from the tensile tests performed on rods A and B of the three batches. The chart shows that, on average, the ultimate strength of both rod A and B decreases for increasing values of build angles, from an average value of 12.11 kN of rod A-X10 up to 8.40 kN of rod B-X30. Table 2 provides, for each batch, the average values and standard deviations of the ultimate strengths of rods A and B as well as their average ratios (strength ratio). First of all, it is with noticing that the coefficient of variation (COV) of the ultimate strengths tends to increase with increasing intersection angles for both rods A (from 0.06 for 10° to 0.11 for 30°) and B (from 0.10 for 10° to 0.24 for 30°). Similarly, the strength ratios tend to increase with increasing values of the intersection angle, from 1.07 for 10° to 1.33 for 30°.

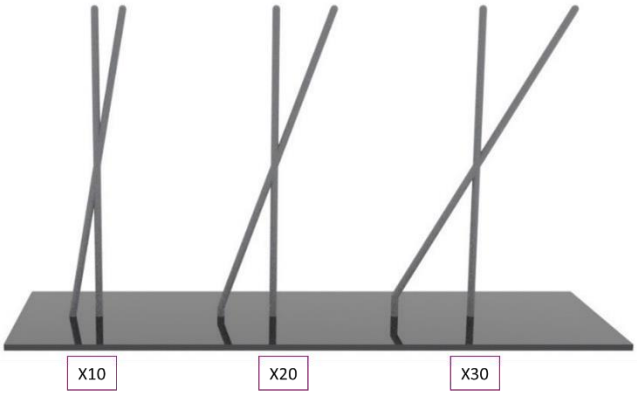

Figure 4 Stainless steel crossed rods with three different build angles, respectively X10, X20, and X30 batches

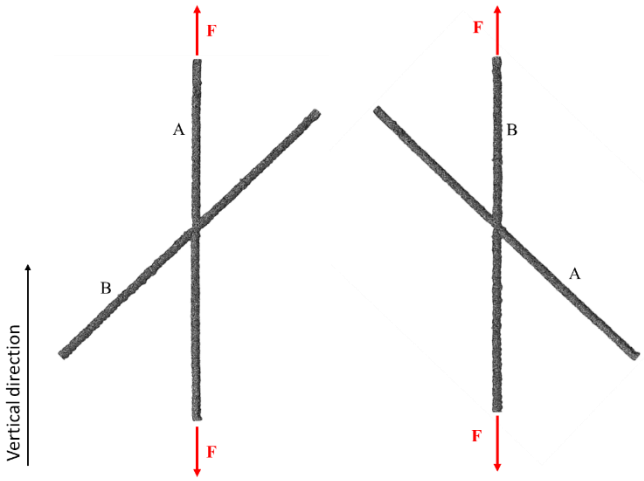

Figure 5 WAAM-produced crossed rods: loading directions

(a) (b)

Figure 6 Tensile test: a) Experimental tensile set-up, b) typical tensile rupture on the tested rod

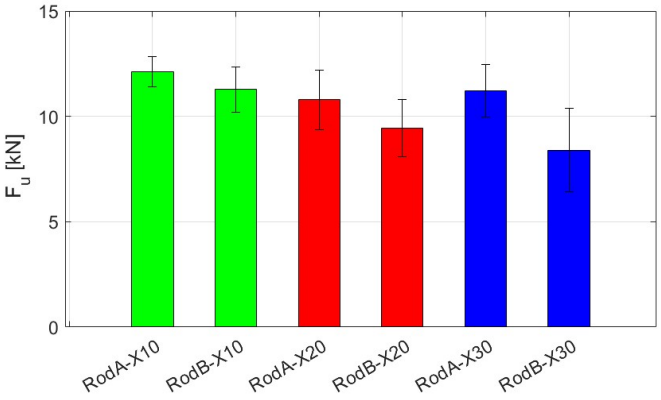

Figure 7 Average values of the ultimate tensile strength of WAAM-produced crossed rods

Table 2 Average values and standard deviations of the ultimate strengths of rods A and B, and their average strength ratio

Specimen ID	$F_{u,rodA}$ [kN]	$F_{u,rodB}$ [kN]	$F_{u,rodA,av}/F_{u,rodB,av}$ [-]
X10	12.11 ± 0.72	11.27 ± 1.09	1.07
X20	10.78 ± 1.40	9.45 ± 1.36	1.14
X30	11.21 ± 1.23	8.40 ± 1.99	1.33

4. Outlook and future work

The present work provides an overview of the first exper-

imental investigations aimed at characterizing the mechanical behavior of WAAM-produced stainless steel single and crossed rods, as basic components of lattice structures, under different loading conditions. The results of the experimental tests on single rods and crossed rods are of fundamental importance to assess the structural performances and design unitary cells and lattice structures manufactured using WAAM dot-by-dot process (Figure 8).

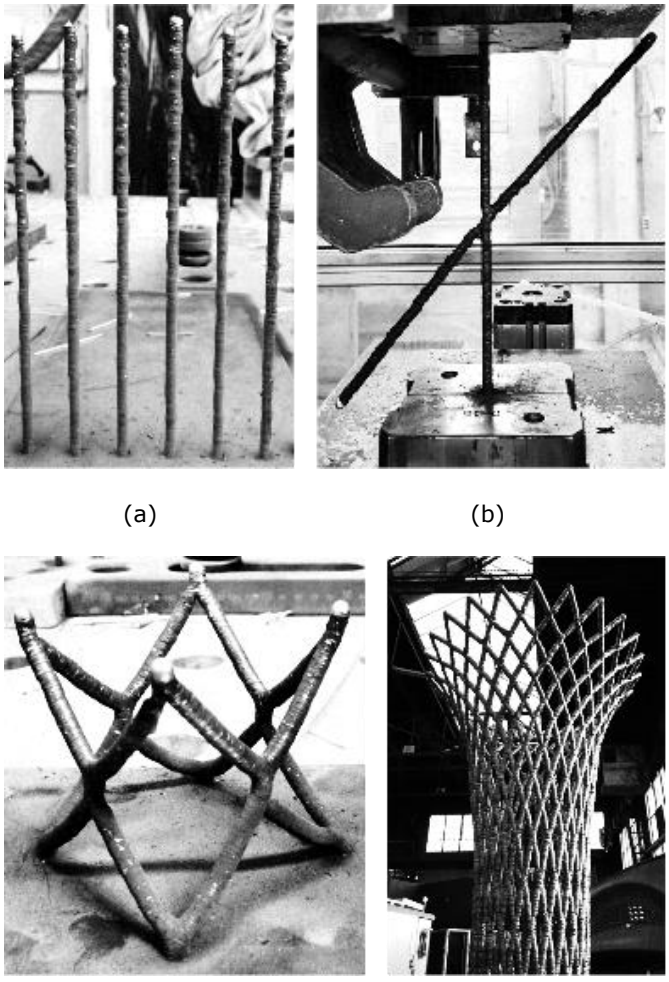

Figure 8 Dot-by-dot WAAM-produced lattice structure components: (a) single rods, (b) crossed rod, (c) unitary cell, (d) lattice structure

The results of the first experimental tests pointed out the following remarks:

- The single rods printed at different build angles exhibited a remarkably different behavior in tension characterized by a significantly lower Young's modulus when compared with that of conventionally manufactured stainless steel parts. On the other hand, this result is in line with the tensile results found in literature for WAAM-produced stainless steel plates.
- The single rods tested under compression loading exhibited a compression capacity that, as expected, decreased with the increase of the rod lengths, following the trends of the buckling curves of conventionally manufactured steel members. The results obtained from the compression tests will be interpreted considering the detailed geometrical characterization obtained from 3D laser scanning, to assess the influence of the geometrical irregularities on the compression response of the printed rods. Ad-hoc buckling curves will be developed, taking into account geometrical and mechanical parameters that affect the global buckling behavior of WAAM-produced rods.
- The tensile behavior of crossed rods is remarkably influenced by the build angle that determined a 30% reduction of the ultimate strength of the rod moving from a build angle of 0° (vertically printed bar) to 30°. Such large ultimate strength reduction should be properly considered in the design phase. Additional studies and analysis, including interpretation of microstructural and fractographic analysis and high-resolution 3D laser scanning, are currently under development to provide a more sound interpretation of the mechanical behavior of "dot-by-dot" WAAM-produced crossed rods.

References

[1] Buchanan, C.; Gardner, L. (2019) *Metal 3D printing in construction: A review of methods, research, applications, opportunities and challenges*. Engineering Structures 180, pp. 332–348. https://doi.org/10.1016/j.engstruct.2018.11.045

[2] Rodrigues, T.A. et al. (2019) *Current status and perspectives on wire and arc additive manufacturing (WAAM).* Materials 12(7), p.1121. https://doi.org/10.3390/ma12071121

[3] Wolf, A.; Rosendahl, P.L.; Knaack, U. (2022) *Additive manufacturing of clay and ceramic building components*. Automation in Construction 133, p.103956. https://doi.org/10.1016/J.AUTCON.2021.103956

[4] Cunningham, C.R. et al. (2018) *Invited review article: Strategies and processes for high quality wire arc additive manufacturing*. Additive Manufacturing 22, pp. 672–686. https://doi.org/10.1016/j.addma.2018.06.020

[5] Gardner, L.; Kyvelou, P.; Herbert, G.; Buchanan, C. (2020) *Testing and initial verification of the world's first metal 3D printed bridge*. Journal of Construction Steel Research 172, p.106233. https://doi.org/10.1016/j.jcsr.2020.106233

[6] Evans, S.I. et al. (2022) *A review of WAAM for steel construction – Manufacturing, material and geometric properties, design, and future directions*. Structures 44, pp. 1506-1522. https://doi.org/10.1016/j.istruc.2022.08.084

[7] Laghi, V. et al. (2023) *Blended structural optimization for wire-and-arc additively manufactured beams*. Progress in Additive Manufacturing 8, pp. 381-392. https://doi.org/10.1007/s40964-022-00335-1

[8] Li, Z. et al. (2022) *Digital and automatic design of free-form single-layer grid structures*. Automation in Construction 133, p.104025. https://doi.org/10.1016/J.AUTCON.2021.104025

[9] Dörrie, R. et al. (2022) *Combined Additive Manufacturing Techniques for Adaptive Coastline Protection Structures*. Buildings 12(11), p.1806. https://doi.org/10.3390/buildings12111806

[10] Dinovitzer, M. et al. (2019) *Effect of wire and arc additive manufacturing (WAAM) process parameters on bead geometry and microstructure*. Additive Manufacturing 26, pp. 138-146. https://doi.org/10.1016/j.addma.2018.12.013

[11] Evans, S.I.; Xu, F.; Wang, J. (2023) *Material properties and local stability of WAAM stainless steel equal angle sections*. Engineering Structures 287, p.116160. https://doi.org/10.1016/j.engstruct.2023.116160

[12] Kyvelou, P. et al. (2020) *Mechanical and microstructural testing of wire and arc additively manufactured sheet material*. Materials & Design 192, p.108675. https://doi.org/10.1016/j.matdes.2020.108675

[13] Laghi, V. et al. (2022) *Mechanical response of dot-by-dot wire-and-arc additively manufactured 304L stainless steel bars under tensile loading*. Construction and Building Materials 318, p.125925 https://doi.org/10.1016/j.conbuildmat.2021.125925

[14] MX3D, www.mx3d.com.

[15] European Committee for Standardization (CEN) (2015) *EN 1993 1-4: Eurocode 3 - Design of steel structures, part 1-4: General rules, supplementary rules for stainless steel*.